Early Periimplant Tissue Healing on 1-Piece Implants With a Concave Transmucosal Design: A Histomorphometric Study in Dogs

Caroline Bolle, DDS,* Marie-Paule Gustin, DS, PhD,† Didier Fau, DVM, PhD,‡ Patrick Exbrayat, DDS,§ Georges Boivin, PhD,¶ and Brigitte Grosgogeat, DDS, PhD||

Introduction: *The purpose of our study was to investigate the early healing phase of marginal bone and soft tissues around unloaded 1-piece implants with a concave transmucosal design, in a dog model.*

Methods: *Twenty-four 1-piece implants with a concave transmucosal neck were inserted 1 mm subcrestally in the mandibular ridge of 8 beagle dogs. Four animals were sacrificed after 3 and 12 weeks of healing. Histomorphometric analysis was performed to measure the height of the periimplant tissues.*

Results and Discussion: *The overall height of the periimplant mucosa was, respectively, 2.67 and 2.52 mm, after 3 and 12 weeks. In the connective tissue, a soft tissue O-ring seal was observed in the healing area provided by the transmucosal concavity, after 12 weeks. The location of the first bone-to-implant contact facing the implant shoulder was 0.00 and +0.18 mm, respectively, after 3 and 12 weeks of healing. Some bone apposition occurred on the implant shoulder during the healing.*

Conclusion: *Within the limits of the present study, a concave transmucosal design in 1-piece implants was associated with a short vertical value of biological width and promoted a mechanical interlocking of the implant body at the connective tissue and marginal bone levels. (Implant Dent 2015;24:1–9)*

Key Words: narrow transmucosal design, biological width, histomorphometry, dental implant

The achievement of an adequate mucosal attachment and marginal bone preservation during early healing are essential to ensure long-term aesthetic and functional success for implant-supported rehabilitations.

Periimplant mucosa is an efficient protective seal between the oral environment and the osseointegrated part of the implant. The formation and maturation of this soft tissue barrier require 6 to 12 weeks after implant surgery.[1] A minimum width of periimplant soft tissue—called biological width—is required, and during the healing, bone loss may occur to accommodate the soft tissues until the adequate dimensions are restored.[2] The marginal level of the mucosa, which is essential for good aesthetics, also depends on the level of the underlying bone support. There is a real interaction between the mucosa, as a protective seal for osseointegration, and the marginal periimplant bone supporting the mucosa.

The characteristics of an implant transmucosal design (connections, platforms, surface properties) are related to biological width dimensions, marginal periimplant bone levels, and the amount of inflammation in the periimplant soft tissue. For years, 2 design parameters have been identified as crucial during the first weeks of healing. First of all, a microgap at the implant-abutment interface of 2-part implants creates an inflammatory process due to micromovement and bacterial infiltration,[3–5] leading to marginal bone loss,[6–8] biological width lengthening, and marginal recession[9] when the implant/abutment interface was positioned at bone level or subcrestally. Furthermore, a "smooth"

*Student PhD, Laboratoire des Multimatériaux et Interfaces UMR CNRS 5615, Université Lyon 1, Université de Lyon, Villeurbanne, France; Assistant Professor, Université de Rennes 1, Faculté d'Odontologie, Université Européenne de Bretagne, Rennes, France; Hospital Practitioner, CHU de Rennes, Pôle d'Odontologie et de Chirurgie Buccale, Rennes, France.
†Associate Professor, Department of Public Health, Institute of Pharmacy (ISPB), EA4173, Université Lyon 1, Université de Lyon, Lyon, France; Hospital Practitioner, Service de Biostatistiques, Hospices Civils de Lyon, Lyon, France.
‡Professor, Interactions Cellule Environment UPSP ICE 2011-03-101, Vet Agro Sup, Université de Lyon, Marcy l'Etoile, France.
§Associate Professor, UFR Odontologie, Université Lyon 1, Lyon, France; Hospital Practitioner, Service de Consultations et de Traitements Dentaires, Hospices Civils de Lyon, Lyon, France.
¶Research Director, INSERM, UMR 1033, Université de Lyon, Lyon, France.
||Professor, Laboratoire des Multimatériaux et Interfaces UMR CNRS 5615, UFR Odontologie, Université Lyon 1, Université de Lyon, Lyon, France; Hospital Practitioner, Service de Consultations et de Traitements Dentaires, Hospices Civils de Lyon, Lyon, France.

Reprint requests and correspondence to: Caroline Bolle, DDS, Laboratoire des Multimatériaux et Interfaces (UMR CNRS 5615), Faculté d'Odontologie de Lyon, 11 Rue Guillaume Paradin, 69372 Lyon Cedex 08, France, Phone: +33-4-78-77-86-89, Fax: +33-4-78-77-87-13, E-mail: caroline.bolle@univ-rennes1.fr

ISSN 1056-6163/15/02405-001
Implant Dentistry
Volume 24 • Number 5

DOI: 10.1097/ID.0000000000000301

surface of the endosseous part of the implant collar is responsible for early marginal periimplant bone loss[7,10] and biological width lengthening.[9]

More recently, the influence of the transmucosal component design on periimplant soft tissue integration and marginal bone remodeling has been suggested. Conventional flared transmucosal components might compress and weaken the periimplant mucosa, whereas concave transmucosal designs may promote the adhesion, thickness, and mechanical properties of the connective tissue.[11] A narrow transmucosal design increases the length of the implant-tissue contact and provides a horizontal healing space for the connective tissue, which might reduce the height required for biological width and subsequently the marginal bone loss due to soft tissue adaptation.[11–13]

According to Rompen et al,[13] in a pilot clinical study, a concave transmucosal profile in 2-part implants led to a better and more predictable soft tissue stability in the aesthetic zone compared to the previous published data on implants with a divergent transmucosal design.

Only 2 histologic studies have been recently carried out to investigate this implant design with a supracrestal implant-abutment interface.[14,15] Both authors reported lower amounts of bone resorption on concave transmucosal profiles compared to straight profiles. However, controversial outcomes were reported about periimplant mucosa dimensions. According to Kim et al,[14] the vertical dimensions of the periimplant mucosa were similar on concave, straight, or flared transmucosal 1-piece implants after 6 months of unloaded healing in the beagle dog, whereas Huh et al[15] reported that a concave transmucosal design led to lower biological width vertical values compared to straight profiles after 16 weeks of loaded healing in the beagle dog.

Therefore, the aim of the present study was to investigate the effect of a concave transmucosal design of 1-piece implants on periimplant mucosa maturation, dimensions, collagen fiber organization, and marginal bone levels after 3 and 12 weeks of healing in the beagle dog.

MATERIALS AND METHODS

Animals

The experimental protocol was approved by the Committee of Ethics of the National Veterinary School of Lyon (VetagroSup), and the surgical procedures were performed at the Claude Bourgelat Institute, a specific center for preclinical trials.

Eight young adult beagle dogs (10–12 months old and approximately 10 kg) were included in this study according to the ARRIVE guidelines.[16] The experimental part of the study started after an adaptation period of 2 weeks. At the beginning of the study, all animals exhibited a fully erupted permanent dentition. After tooth scaling, a plaque control program was initiated, consisting of cleaning with a soft toothbrush (Méridol; GABA, Bois Colombes, France) and 0.20% chlorhexidine gel (Elugel; Pierre Fabre, Castres, France) 3 times per week during the whole experimental period. The dogs were fed with a soft diet and water and were housed in cages of 2 for the entire duration of the experiment.

Implants

A commercially available sandblasted Ti-6Al-4V implant (TwinKon implant, Tekka; Global D, Brignais, France) was selected according to the concave configuration of its transmucosal neck (Fig. 1). This implant has a 1-piece design with a concave transmucosal collar and an external conical connection located above the collar. The external conical connection is protected with a PEEK plastic ring. The concave transmucosal part is 1.5 mm high and 1.73 mm long. The horizontal inward mismatch between the implant body and the transmucosal component is 0.4 mm. The selected implants were 8.5 mm long, with a conicocylindrical screw-type shape (∅3.5 mm). The sandblasted surface (sprayed with corundum micropowder) extends to the apical portion (0.20 mm high) of the transmucosal neck. The coronal portion of the transmucosal neck is machined (1.3 mm high).

Surgical Procedure

The study was performed in 2 surgical steps. At the beginning of the experiment, all the mandibular premolars were carefully extracted after tooth separation. Following a healing period of 10 weeks, the surgery for implant insertion was performed, using midcrestal incisions and mucoperiosteal flap elevation. Three implants per dog were randomly assigned to the residual mandibular left or right ridge (Fig. 2, A). The opposite sides of the mandibular edentulous ridge were used for another experimental purpose, the results of which will be reported with further data. A total of 24 fixtures were carefully inserted, under profuse irrigation with sterile saline (Versol; Laboratoire Aguettant, Lyon, France), spacing the implants at a distance of 10 mm apart. The implant body shoulder was positioned with good primary stability 1 mm subcrestally. Implant healing abutments were connected immediately following implant placement. The flaps were repositioned and sutured with 4-0 braided absorbable sutures (Vicryl; Ethicon Inc., Johnson & Johnson, New Brunswick, NJ). During the 10 days following each surgery, the toothbrushing program (3 times per week) was replaced by daily spraying with 0.20% chlorhexidine (Eluspray; Pierre Fabre). Sutures were removed 10 days after surgery. The animals were divided into 2 groups, with 4 animals in each group, according to the healing periods: 3 and 12 weeks.

All surgical procedures were performed under general anesthesia and sterile conditions. For premedication purposes, the animals were injected with a cocktail of benzodiazepine

Fig. 1. TwinKon implant has a 1-piece design with a concave transmucosal neck.

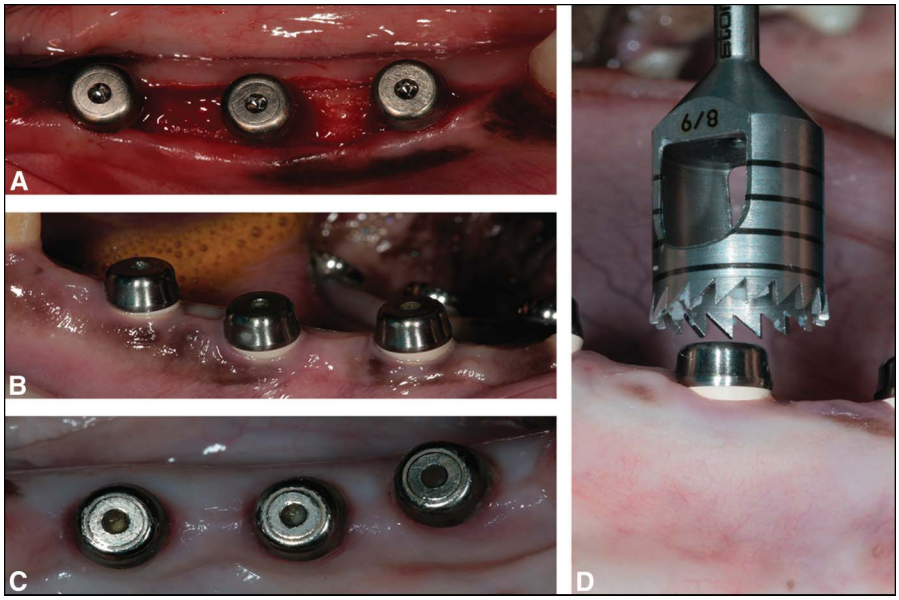

Fig. 2. Implants in the left side of the alveolar mandibular ridge: (**A**) after insertion, (**B**) after 3 weeks of healing, (**C**) after 12 weeks of healing, and (**D**) harvesting with a trephine.

(0.5 mg/kg; Valium Roche 5 mg; Roche, Boulogne-Billancourt, France), acepromazine (0.1 mg/kg; Vétranquil; Ceva Sante Animale, Libourne, France), and glycopyrrolate (0.01 mg/kg; Robinul; Vétoquinol, Paris, France). General anesthesia was induced intravenously with ketamin (5 mg/kg; Imalgène 1000; Mérial, Lyon, France) and maintained using isoflurane inhalation (Vetflurane; Virbac, Carros, France). The animals were monitored with an electrocardiogram (Dynascope DS 7100; Fukuda Denshi, Tokyo, Japan) during the procedures. For pain control, the animals received 3 intravenous injections of morphine (Morphine chlorohydrate Lavoisier; Laboratoire Chaix et Du Marais, Paris, France): for premedication, at the end of the procedure, and 4 hours after the extubation (0.2 mg/kg). In addition, a fentanyl transcutaneous patch (Durogésic; Janssen-Cilag, Issy-les-Moulineaux, France) was placed on the day of surgery (75 μg/h), and meloxicam (Métacam; Boehringer-Ingelheim, Reims, France) was given to the animals for 10 days (0.2 $mg \cdot kg^{-1} \cdot j^{-2}$ the first day and 0.1 $mg \cdot kg^{-1} \cdot j^{-2}$ the next 9 days). To prevent any infection, the dogs received a combination of amoxicillin and clavulanic acid (Augmentin; Laboratoire GlaxoSmithKline, Marly-le-roi, France) twice a day for 10 days (200 mg/50 mg).

At the end of the healing period, the animals were sacrificed with an overdose of pentobarbital (Doléthal; Vétoquinol). The fixtures and surrounding hard and soft tissues were then carefully harvested using a trephine (Stoma; Storz am Mark GmbH, Emmingen-Liptingen, Germany) with an inner diameter of 10 mm, under irrigation (Fig. 2, D).

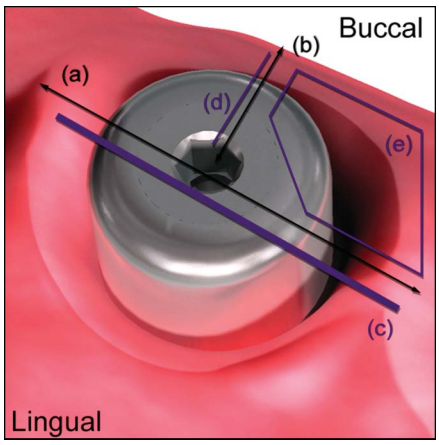

Fig. 3. Sectional drawing used for the histological process: (a) mesiodistal section, (b) buccolingual section of the buccal remaining bloc, (c) mesiodistal ground section (modified Paragon staining), (d) vertical buccal thin (Goldner trichrome staining) and ultrathin sections, (e) horizontal proximobuccal thin section (toluidine blue staining).

Histological Preparation and Analysis

The samples were immediately fixed in 2% glutaraldehyde and 2% paraformaldehyde in a sodium cacodylate buffer for 1 week. Dehydration was performed in serial steps of ethanol concentrations, and the blocks were finally embedded in methyl methacrylate (Merck KGaA, Darmstadt, Germany).

Nondecalcified sections were prepared using a method adapted from Donath and Breuner.[17] The polymerized blocks were cut in the mesiodistal plane parallel to the long axis of each implant (Fig. 3, a), using a diamond wire saw (Well 3242; Well Diamond Wire Saws Inc., Norcross, GA). One central mesiodistal section (Fig. 3, c) was obtained and reduced by microgrinding and polishing, starting from the lingual part of each block, to a thickness of about 40 μm, using an Exakt grinding unit (Exakt Advanced Technologies GmbH, Norderstedt, Germany). The ground sections were then superficially stained with a modified Paragon, and the histomorphometric quantification was performed at different magnifications, using a light microscope (Zeiss Axioskop; Carl Zeiss SMT GmbH, Oberkochen,

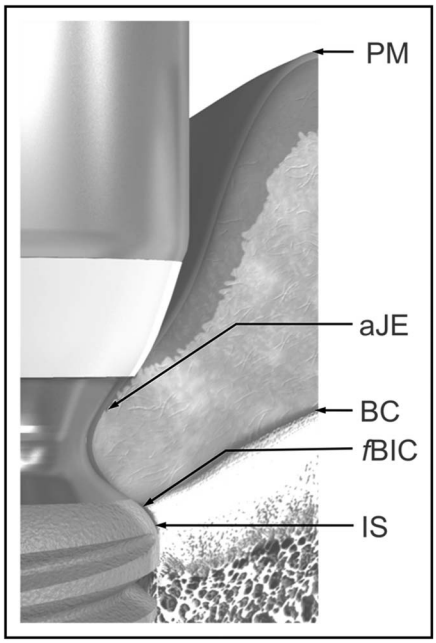

Fig. 4. Landmarks used for the histomorphometric measurements: IS, *f*BIC, the top of the BC, PM, and the aJE.

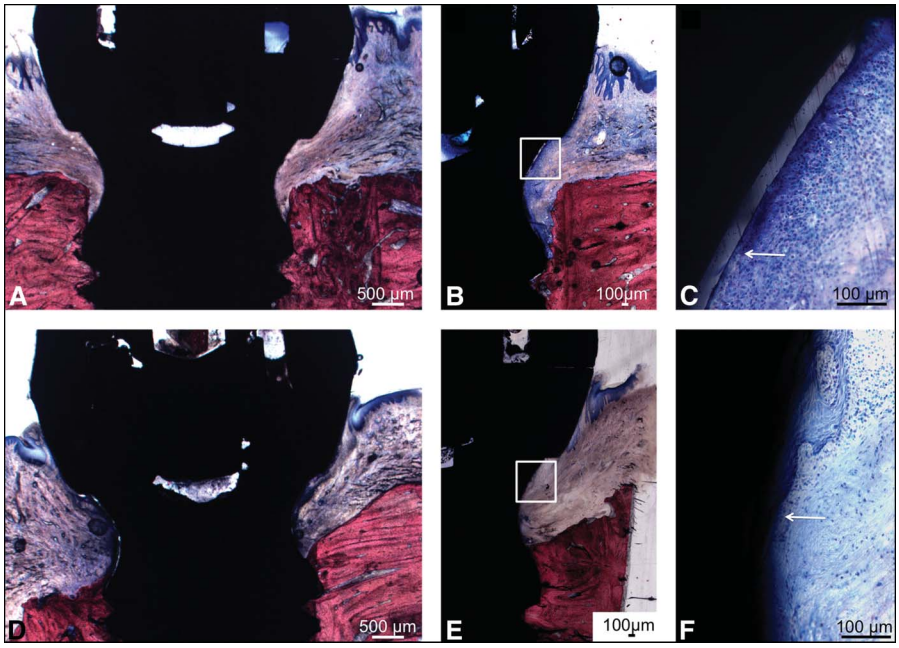

Fig. 5. Ground nondecalcified mesiodistal sections. **A**, **B**, **C** (details of **B**): After 3 weeks of healing, a nonkeratinized junctional epithelium is observed facing the titanium surface. **D**, **E**, **F** (details of **E**): After 12 weeks of healing, the junctional epithelium was in close contact with the titanium surface, a dense connective tissue was interposed between the apical extent of the junctional epithelium and the most coronal bone-to-implant contact. Light microscopy, modified Paragon staining. White arrow indicates the apical extend of the junctional epithelium.

Germany) equipped with an imagery digital software (Bone Morpho Expert; Explora Nova, La Rochelle, France).

For each section, the marginal portion of the mucosa (PM), the apical extent of the junctional epithelium (aJE), the first bone-to-implant contact (*f*BIC), the implant shoulder (IS), and the top of the bone crest (BC) were identified at both the mesial and the distal sides of the sections and used for the linear measurements, thus resulting in 2 measured sites per implant (Fig. 4). The vertical distances between the landmarks were determined in a direction that was parallel to the long axis of the implant and expressed in millimeters for PM-aJE, aJE-*f*BIC, PM-*f*BIC, IS-BC, IS-*f*BIC, and BC-*f*BIC. The length of the soft tissue was also measured according to the shape of the soft tissue-implant interface (PM-aJE length, aJE-CLB length, PM-*f*BIC length).

The buccal parts of each block were cut buccolingually and parallel to the long axis of the implant (Fig. 3, b) using a diamond wire saw. The implants were mechanically removed, and the residual blocks were re-embedded in methyl methacrylate fast and cold curing resin (Technovit 3040; Heraus Kulzer GmbH, Wehrheim, Germany) and processed to obtain thin nondecalcified histological sections (about 8 µm), using a microtome (Leica SM2500; Leica Biosystems GmbH, Nussloch, Germany). Vertical sections were performed parallel to the long axis of the concave abutment, resulting in buccal thin sections (Fig. 3, d), and were stained with Goldner trichrome. Horizontal sections were performed perpendicular to the concave abutment (in the small axis of the implant) (Fig. 3, e) and were stained with toluidine blue. These sections were then observed at different magnifications; using a light microscope (Zeiss Axioskop; Carl Zeiss SMT GmbH) equipped with an imagery digital software (Bone Morpho Expert; Explora Nova). Identical methodological procedures are reported by Boivin and Meunier.[18]

In the remaining part of the buccal blocks, ultrathin vertical sections (approximately 70 nm thick) were cut in the connective tissue using a Reichert ultracut E (Leica Microsystems GmbH, Wetzlar, Germany) ultramicrotome (Fig. 3, d). These sections were mounted on 200 mesh copper grids coated with 1:1.000 poly-lysine, stabilized for 1 day at room temperature (RT), and contrasted with uranyl acetate and lead citrate. Sections were observed using a Jeol JEM-1400 (Jeol Ltd., Tokyo, Japan) transmission electron microscope operating at 80 kV, equipped with an Orius-600 camera (Gatan Inc., Pleasanton, CA) and with an imagery digital software (DigitalMicrograph; Gatan Inc.). Electron micrographs were obtained from the connective tissue in the 200 µm segment next to the implant collar surface.

Statistical Method

A power analysis was conducted to determine the number of dogs required to detect population differences corresponding to a large Cohen[19] effect size ($\geq$1) between the 2 healing periods, whatever the variables. The power was set at 90% and the significant level *P* at 5%. For an adequate implant distribution, 3 implants per animals with 2 replicates (mesial and distal views) were placed, thus allowing 6 observations per animal.

To study the healing period effect on each of the variables, we took into account the hierarchical data structure (view/location/dog), and we performed for each variable a 3-level mixed-effects model. Only the intercept was considered random assuming that the effect of the healing period on the outcome was independent from the dog and the location.

A significant level of 5% was selected. Statistics were performed using the R language, version 3.0.2., available on the http://cran.r-project.org/ Web site. The function pwr.t.test of the R package pwr was used for the power analysis and the function lme of the R package nlme for the mixed-effects models. In case of missing data, they were supposed to be missing completely at random, and no data imputation was performed. Data distribution normality was checked graphically and using the normality Shapiro-Wilk test.

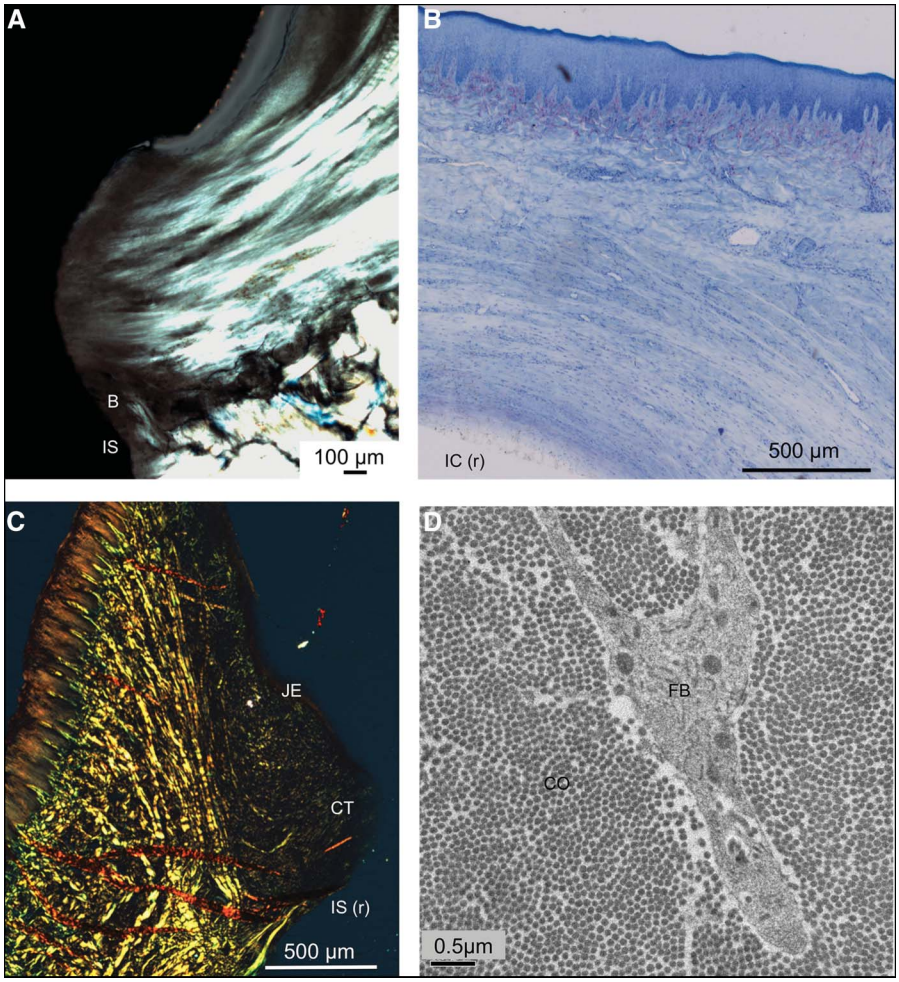

Fig. 6. Organization of collagen fibers within the connective tissue after 12 weeks of healing. **A**, In the connective tissue located outside the implant concavity, collagen fibers are inserted into the crestal bone and run perpendicularly to the abutment (light polarized microscopy, modified Paragon staining, ground nondecalcified vertical mesiodistal section). IS indicates implant shoulder; B, periimplant marginal bone. **B**, Closer to the implant surface, a concentric organization of the collagen fibers was observed with a width of about 500 µm in the transversal (horizontal) plane around the concave part (light microscopy, thin proximobuccal horizontal section, toluidine blue staining). IC (r) indicates implant collar removed. **C**, In the implant collar concavity, thin vertical buccal sections showed collagen fibers cut transversely in the connective tissue (light polarized microscopy, Goldner trichrome staining). CT indicates connective tissue; IS (r), implant shoulder removed; JE, junctional epithelium. **D**, In the connective tissue close to the implant collar, ultrathin vertical buccal section showed collagen fibers cut transversely (electron micrograph). CO indicates collagen fiber; FB, fibroblast.

RESULTS

Clinical Observations

The postoperative healing was uneventful for all implants, and no complication was noted during the whole follow-up period. After 3 weeks, the soft tissue healing process seemed to be well advanced with good wound closure (Fig. 2, B). No clinical sign of periimplant mucosa inflammation was observed. After 12 weeks, the periimplant mucosa seemed to be clinically mature. A slight redness of the mucosa was observed both on the abutments and on the remaining teeth (Fig. 2, C). All 24 implants were clinically osseointegrated.

Histological Observations

Soft tissue healing. After 3 weeks of healing, a nonkeratinized epithelium was formed. The connective tissue exhibited some signs of organization with numerous fibroblasts disposed along the axis of the collagen fibers. Minor inflammatory infiltrated areas were observed in the connective tissue along the sulcular epithelium (Fig. 5, A–C).

After 12 weeks, the tissue maturation and collagen bundle organization were achieved. The junctional epithelium was mature and in close contact with the titanium surface. The extent of the junctional epithelium was located in the coronal part of the concave abutment below the PEEK ring. Areas of inflammation were regularly detected in the connective tissue adjacent to the junctional epithelium extending as far as the implant-PEEK apical junction. A dense connective tissue in close contact with the titanium surface in the collar concavity was interposed between the apical extent of the junctional epithelium and the marginal bone (Fig. 5, D–F). This connective compartment was devoid of inflammatory infiltrate.

Collagen fiber orientation in the connective tissue after 12 weeks. The connective tissue was rich in fibroblasts and collagen fibers that were inserted into the crestal bone and running toward the abutment in a horizontal and convergent direction (Fig. 6, A).

Closer to the implant collar, in the thin histological horizontal sections, a circular organization of the collagen fibers was detected in the horizontal healing space provided by the transmucosal concavity, with a width of about 500 µm (from the implant collar toward the periphery) in the transversal (horizontal) plane (Fig. 6, B). The thin and ultrathin vertical sections showed collagen fibers cut transversely, suggesting a parallel circumferential arrangement of the collagen fibers around the concave collar (Fig. 6, C and D).

Marginal bone remodeling. After 3 weeks of healing, intense bone apposition on the implant surface and crestal bone remodeling were ongoing. The first bone-to-implant contact was located at the implant shoulder. Woven bone was detectable on the old bone bed at the marginal level but away from the

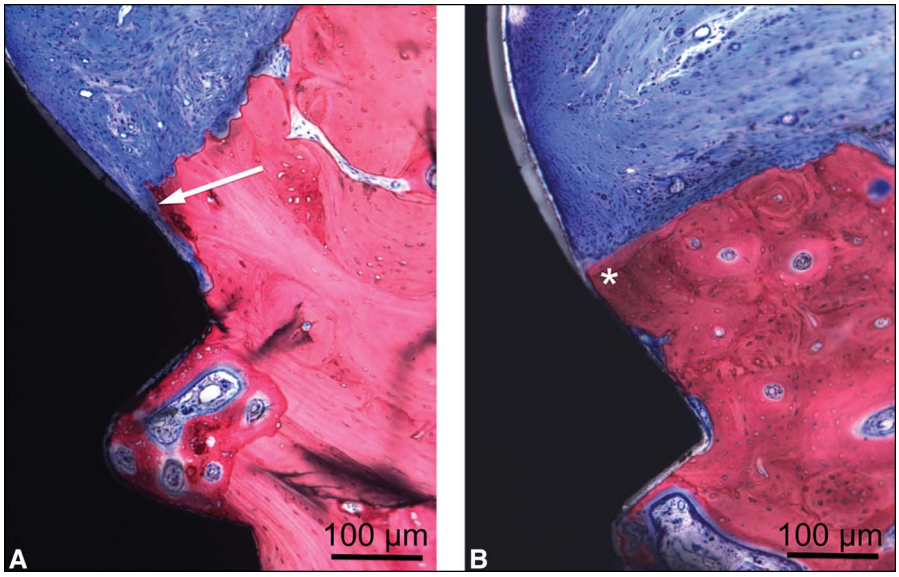

Fig. 7. Marginal bone healing. **A**, After 3 weeks, the first pitch of the implant thread was in contact with the old bone bed (light pink). Woven bone (dark pink) was observed along the old bone bed. **B**, After 12 weeks, the new bone had established the most coronal contact with the implant body. Light microscopy, modified Paragon staining, mesiodistal nondecalcified ground sections. Arrow indicates old bone bed, and asterisk indicates woven bone.

implant shoulder (Fig. 7, A). The first pitch of the implant thread was still in contact with the old bone bed.

After 12 weeks, the crestal remodeling and osseointegration processes were completed. New bone had established the most coronal contact with the implant body (Fig. 7, B).

Histomorphometrical Measurements

A sample of 4 dogs per group was determined to have sufficient power. Each of the 8 dogs was sampled according to a healing period (3 or 12 weeks). For each dog, 3 locations on the arch were selected (anterior, middle, and posterior), and for each location, 2 measurements were replicated on each view (mesial/distal), thus providing 48 observations for 9 variables (PM-aJE, aJE-*f*BIC, PM-*f*BIC, IS-BC, IS-*f*BIC, BC-*f*BIC, PM-aJE length, aJE-CLB length, and PM-*f*BIC length). Three observations were missing for 6 variables. Data for the histomorphometric measurements are summarized in Table 1.

Table 1. Results From the Histomorphometric Measurements of the Epithelial Tissue (PM-aJE), Connective Tissue (aJE-*f*BIC), Biological Width (PM-*f*BIC), Periimplant Crestal and Marginal Bone Levels (IS-*f*BIC, BC-*f*BIC, and IS-BC)

Implant Group	n	IS-*f*BIC	BC-*f*BIC	IS-BC
3 wk	24	**0.00** (0.43)	**–0.93** (0.61)	**0.93** (0.64)
12 wk	24	**0.18** (0.12)	**–0.72** (0.44)	**0.89** (0.47)
Implant Group	**n**	**PM-aJE**	**aJE-*f*BIC**	**PM-*f*BIC**
3 wk	21	**1.36** (0.42)	**1.42** (0.50) ↕	**2.78** (0.57)
12 wk	24	**1.87** (0.51)	**0.65** (0.14) ↕	**2.52** (0.47)
Implant Group	**n**	**PM-aJE Length**	**aJE-*f*BIC Length**	**PM-*f*BIC Length**
3 wk	21	**1.58** (0.53) ↕	**1.62** (0.62) ↕	**3.20** (0.59)
12 wk	24	**2.38** (0.53) ↕	**0.69** (0.15) ↕	**3.07** (0.48)
Implant Group	**n**	**d (L/h) PM-aJE**	**d (L/h) aJE-*f*BIC**	**d (L/h) PM-*f*BIC**
3 wk	21	**0.22** (0.18) ↕	**0.20** (0.19) ↕	**0.42** (0.19) ↕
12 wk	24	**0.51** (0.07) ↕	**0.05** (0.03) ↕	**0.55** (0.09) ↕

Data are expressed in millimeters, as average and standard deviation; n indicates number of measured sites, ↔$P \leq 0.05$.

Dimensional changes of the periimplant mucosa. The PM-aJE was much longer after 12 weeks of healing (1.87 vs 1.36 mm after 3 weeks), the decrease of aJE-*f*BIC was statistically significant ($P = 0.01$) with 1.42 and 0.65 mm at 3 and 12 weeks of healing, respectively, and the PM-*f*BIC was shorter after 12 weeks of healing (2.78 and 2.52 mm at 3 and 12 weeks, respectively); however, the difference was not significant.

The relationship between the epithelium and the connective tissue, components of the biological width, are presented in Figure 8. After 3 weeks of healing, the epithelial barrier represented about 49% of the transmucosal interface, whereas after 12 weeks of healing, the epithelial compartment represented 74% of the transmucosal vertical dimensions.

After 3 weeks, the PM-*f*BIC length was 3.20 mm with a PM-aJE length of 1.58 mm and a aJE-*f*BIC length of 1.62 mm. After 12 weeks, the PM-*f*BIC length was 3.07 mm with a PM-aJE length of 2.38 mm and an aJE-*f*BIC length of 0.69 mm. The difference between the length of the epithelium and the connective tissue recorded at the 2 periods was statistically significant ($P = 0.02$ and $P = 0.01$).

The difference between the length and height of the epithelial tissue, connective tissue, and biological width after 3 and 12 weeks were statistically significant (respectively, $P = 0.00$, $P = 0.04$, and $P = 0.05$). After 3 weeks, the difference between the length and height of the biological width was 0.42 mm, whereas it was 0.55 mm after 12 weeks.

Marginal and crestal bone levels. The BC-*f*BIC was –0.93 mm after 3 weeks of healing and –0.72 mm after 12 weeks. A crestal bone remodeling

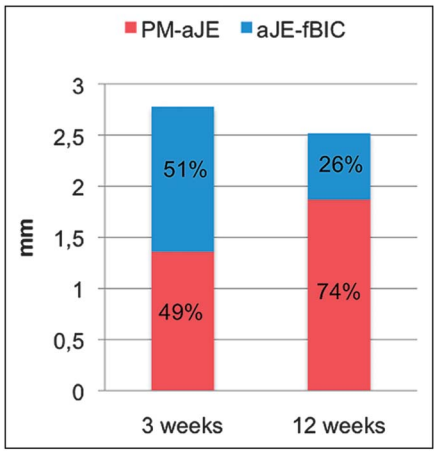

Fig. 8. Histogram representing the vertical distribution of the tissue above the implant shoulder after 3 and 12 weeks of healing. Epithelial (red) and connective (blue) tissues, dimensions expressed in millimeters.

occurred during the healing. After 12 weeks, the location of the first bone-to-implant contact was 0.18 mm. The marginal bone was located above the implant shoulder in 96% of the sections. Some bone apposition occurred on the implant shoulder during the healing.

The marginal bone level was located more coronally after 12 weeks of healing compared to the 3-week period (average: 0.18 vs 0.00 mm), but the difference was not statistically significant.

DISCUSSION

This experimental study evaluated the influence of a concave transmucosal design of 1-piece implants on soft tissue maturation, dimensions, collagen fibers organization, and periimplant marginal bone levels after 3 and 12 weeks of healing in the beagle dog.

In the present investigation, after 3 weeks, the mucosa healing was still ongoing, a nonkeratinized junctional epithelium was formed, and a connective tissue was interposed between the apical extent of the junctional epithelium and the crestal bone. An epithelial downgrowth and a decrease of the connective tissue compartment occurred during the healing. After 12 weeks, tissue maturation and collagen bundle organization were completed. The periimplant mucosa dimensions were similar after 3 and 12 weeks. The healing dynamics were similar to the dynamics reported on 1-piece implants with flared profiles by Berglundh et al.[1] These authors reported that the height of the periimplant mucosa varied from 3.1 to 3.5 mm between 2 and 12 weeks of healing, thus remaining almost the same. A junctional epithelium started to form after 2 weeks and extended in an apical direction until 6 weeks of healing, whereas the connective tissue compartment decreased. According to these authors, soft tissue maturation required 6 to 8 weeks of healing. During our study, we observed that the healing was completed after 12 weeks. However, according to the results published in the literature,[1] it is possible that the healing was completed before this delay, even though no observation was recorded between 3 and 12 weeks, which would have allowed to check and/or confirm the data.

In the present experimental study, vertical values of periimplant mucosa were less than 3 mm after 3 and 12 weeks (respectively, 2.78 and 2.52 mm). These values were lower compared to previous findings on 1-piece implants.

Indeed, Hermann et al[9] reported that the dimensions of the periimplant mucosa on 1-piece cylindrical implants was 3.57 mm when the rough/smooth border was located 1 mm subcrestally, and 2.84 mm when the rough/smooth border was located at bone crest level after 6 months of unloaded healing. Kim et al[14] reported no difference in soft tissue vertical values on concave, straight, or flared transmucosal profiles after 6 months of unloaded healing, with the following values of 2.72 (straight), 2.91 (narrow), and 3.04 mm (flared). However, Huh et al[15] reported lower periimplant mucosa heights on concave transmucosal profiles (2.36 mm) compared to straight transmucosal profiles (2.88 mm) after 16 weeks of healing, but the results were not statistically significant. These propensities are in accordance with the present findings.

In the same way, Finelle et al,[20] in a beagle dog model, compared the bone apposition on the implant shoulder of implants with narrow and wide abutments, using a micro-CT analysis. According to the authors, narrow abutments provide more space to accommodate the biological width, thus reducing the marginal bone remodeling.

Furthermore, after 12 weeks of healing, the inwardly narrowed profile led to a length of mucosa/implant interface of 3.07 mm with a reduced vertical value of 2.52 mm. The length of 3.07 mm is close to previous vertical values of biological width reported on 1-piece implants with a straight or flared transmucosal part.[9]

Finally, our findings, when compared to the data published in the literature, suggest that the horizontal area of a concave transmucosal design increases the length and the surface area of contact at the tissue-implant interface and thus reduces the vertical area required for the biological width.

In the present study, after 12 weeks of healing, the height of the epithelial tissue in the soft tissue interface was increased compared to previously reported data (Berglundh et al[1]). The epithelial compartment represented 74% of the transmucosal vertical dimensions, whereas it was about 60% in the study by Berglundh et al[1] and about 55% (recalculated datum) in the study by Hermann et al[9] on 1-piece cylindrical implants with the rough/smooth border located at bone level or 1 mm subcrestally. Looking closer, after 12 weeks of healing, the vertical value for the connective tissue compartment was short compared to previously reported data: 0.65 mm versus about 1 to 1.5 mm in the literature, whereas the height of the epithelium compartment was closer to previous findings (1.87 vs 1.5–2 mm).

The concave transmucosal abutment may possibly lead to a reduction of the connective tissue compartment in relation with the concavity, thus resulting in a modification of the vertical distribution of epithelial and connective tissues, components of the biological width. Therefore, the old paradigm about the need for a sufficient height of implant/connective tissue contact to prevent bacterial invasion, epithelial downgrowth, or mucosa mechanical breakdown might be jeopardized. Using a transmucosal concave design may change our way of thinking in terms of

surface of contact rather than height of contact. Clinically, the rules for coronoapical positioning of the implants could be simplified. The opportunity to have a reduced biological width with lower connective tissue vertical values might allow a reduced depth positioning of the implant shoulder without the bone remodeling associated with biological width reformation.

According to our findings, collagen fibers in the connective tissue run perpendicular to the abutment and form a soft tissue O-ring seal in the horizontal healing area provided by the transmucosal concavity, after 12 weeks, with a width of about 500 μm in the transversal plane.

The presence of a circular organization of the collagen fibers around the transmucosal component has been reported in the literature for years, but the exact location of these fibers in relation to the abutment and the influence of the transmucosal design still remain unclear. Considering the previous studies on circular collagen bundle organization in the periimplant connective tissue, Buser et al[21] described a 50 to 100 μm wide zone of dense circular fibers close to the implant surface on cylindrical 1-part implants after 3 months of unloaded healing. Ruggeri et al[22] introduced the concept of a periimplant "circular ligament" and reported the presence of circular collagen bundles in close contact with the implant neck of 1-piece loaded implants in the monkey model. Rodriguez et al,[23] in a preliminary histological study, described collagen fibers in the connective tissue compartment that were oriented perpendicularly to the abutment and were organized circumferentially close to the implant surface on platform-switched implants. Degidi et al[24] described, in a human histologic case report on 3 loaded implants with a Morse taper connection, collagen bundles that were oriented perpendicularly to the abutment surface up to 200 μm away from the titanium interface and then form a tridimensional network around the abutment.

These data are in agreement with our results. Concave transmucosal profiles may increase the thickness of the circular periimplant network, thus reinforcing the connective tissue adhesion to the titanium implant.

In the present study, after 12 weeks, the crestal remodeling and osseointegration processes were completed. New bone had established the most coronal contact with the implant body. These data are in agreement with those found in the literature. The osseointegration speed is closely related to the implant surface properties.[25] In a histological study performed on the beagle dog, Berglundh et al[26] observe that after 8 to 12 weeks of healing, the periimplant bone is mature around sandblasted, large-grit and acid-etched (SLA Straumann) implants. For sandblasted implants, a 12-week healing period allows to obtain an adequate osseointegration.[27,28]

With regards to periimplant marginal bone levels, our results show that the first bone-to-implant contact was located at the implant shoulder after 3 weeks, and 0.18 mm above after 12 weeks. Bone apposition occurred on the implant shoulder during the healing period up to the coronal limit of the sandblasted surface. These findings are in agreement with previous results after 12 weeks of healing. According to Hermann et al,[7,10] the first bone-to-implant contact on 1-piece implants was positioned at the level of the rough/smooth border. Kim et al[14] reported a first bone-to-implant contact located 0.03 mm under the implant shoulder on 1-piece implants with a concave transmucosal profile. Huh et al[15] reported a reduced amount of bone resorption on concave transmucosal profiles compared to straight profiles: 0.60 versus 1.44 mm below the implant shoulder.

The BC-*f*BIC was −0.93 mm after 3 weeks of healing and −0.72 mm after 12 weeks. The vertical distances between the top of the bone crest and the first bone-to-implant contact were related to the positioning depth of the rough/smooth border (about 1 mm). According to the results of numerous studies, a subcrestal placement of the implant shoulder was associated with crestal bone remodeling.[29,30]

Thus, the concave transmucosal design allowed for bone integration on the implant shoulder without any bone loss due to biological width reformation. It may also promote the convergence of the collagen bundle toward the implant collar and the formation of a thick circular collagen O-ring within the abutment concavity. This mechanical interlocking of the implant at the connective tissue level might improve the mechanical resistance of the connective adhesion to the titanium. The clinical implication of these findings is the following: good integration of the periimplant tissues during early healing is a key factor for success, to achieve long-term healthy mucosa and stable mucosa dimensions, thus preventing periimplantitis and aesthetic failures.

CONCLUSION

The main observations collected from the present study on periimplant marginal tissue healing around 1-piece implants with a concave transmucosal profile are the following:

1. After 3 weeks, the mucosal and periimplant bone healing was still ongoing, whereas at 12 weeks, epithelium, connective tissue, and bone were mature.
2. Vertical values of biological width were shorter on concave transmucosal implants compared to existing data after 3 and 12 weeks of healing.
3. A soft tissue O-ring seal in the horizontal healing area provided by the transmucosal concavity was observed in the connective tissue compartment after 12 weeks of healing.
4. Some bone apposition occurred on the implant shoulder during the healing.

Further studies are needed to corroborate the present findings. The absence of a control group does not allow us to draw a final conclusion. It might be interesting to set up a comparative study between 1-part implants with straight, concave, and flared transmucosal designs with various positioning depths in relation to the bone crest, to confirm these results. Other parameters may also be considered, such as modified surface properties and microgrooves on the transmucosal part of the implant, which, according to the literature, seem to provide a strong connective tissue adhesion to the titanium surface.

Within the limits of the present study, a concave transmucosal design was associated with a short vertical value of biological width and promoted a mechanical interlocking of the implant body at the connective tissue and marginal bone levels.

Disclosure

The authors claim to have no financial interest, either directly or indirectly, in the products or information listed in the article.

Approval

The experimental protocol was approved by the Committee of Ethics of the National Veterinary School of Lyon (VetagroSup), and the surgical procedures were performed at the Claude Bourgelat Institute, a specific center for preclinical trials.

Acknowledgments

The authors address their special thanks to Dr. Jean-François Borel, Dr. Philippe Duchatelard, and the late Dr. Yves Douillard, original co-designers of the TwinKon implant with the Tekka Global D Society, Brignais, France.

The authors appreciated the precious advise of Dr. Carole Auger and Dr. Hélène Follet. The authors are also grateful for the collaboration of the Tekka Global D team. The study was partially supported by a research grant from Tekka, Global D, Brignais, France.

References

1. Berglundh T, Abrahamsson I, Welander M, et al. Morphogenesis of the peri-implant mucosa: An experimental study in dogs. *Clin Oral Implants Res.* 2007;18:1–8.

2. Berglundh T, Lindhe J. Dimension of the periimplant mucosa. Biological width revisited. *J Clin Periodontol.* 1996;23:971–973.

3. King GN, Hermann JS, Schoolfield JD, et al. Influence of the size of the micro-gap on crestal bone levels in non-submerged dental implants: A radiographic study in the canine mandible. *J Periodontol.* 2002;73:1111–1117.

4. Broggini N, McManus LM, Hermann JS, et al. Peri-implant inflammation defined by the implant-abutment interface. *J Dent Res.* 2006;85:473–478.

5. Zipprich H, Weigl P, Lange B, et al. Micromovements at the implant-abutment interface: Measurement, causes, and consequences. *Implantologie.* 2007;15:31–46.

6. Hermann JS, Cochran DL, Nummikovski PV, et al. Crestal bone changes around titanium implants. A radiographic evaluation of unloaded nonsubmerged and submerged implants in the canine mandible. *J Periodontol.* 1997;68:1117–1130.

7. Hermann JS, Buser D, Schenk RK, et al. Crestal bone changes around titanium implants. A histometric evaluation of unloaded non-submerged and submerged implants in the canine mandible. *J Periodontol.* 2000;71:1412–1424.

8. Weng D, Nagata MJ, Bell M, et al. Influence of microgap location and configuration on radiographic bone loss around submerged implants: An experimental study in dogs. *Int J Oral Maxillofac Implants.* 2011;26:941–946.

9. Hermann JS, Buser D, Schenk RK, et al. Biologic width around one and two-piece titanium implants. *Clin Oral Implants Res.* 2001;12:559–571.

10. Hermann JS, Jones AA, Bakaeen LG, et al. Influence of a machined collar on crestal bone changes around titanium implants: A histometric study in the canine mandible. *J Periodontol.* 2011;82:1329–1338.

11. Touati B, Rompen E, Van Dooren E. A new concept for optimizing soft tissue integration. *Pract Proced Aesthet Dent.* 2005;17:711–712, 714–715.

12. Lazzara RJ, Porter SS. Platform switching: A new concept in implant dentistry for controlling post-restorative crestal bone levels. *Int J Periodontics Restorative Dent.* 2006;26:9–17.

13. Rompen E, Raepsaet N, Domken O, et al. Soft tissue stability at the facial aspect of gingivally converging abutments in the esthetic zone: A pilot clinical study. *J Prosthet Dent.* 2007;97:S119–S125. Erratum in: *J Prosthet Dent.* 2008;99:167.

14. Kim S, Oh KC, Han DH, et al. Influence of transmucosal designs of three one-piece implant systems on early tissue responses: A histometric study in beagle dogs. *Int J Oral Maxillofac Implants.* 2010;25:309–314.

15. Huh JB, Rheu GB, Kim YS, et al. Influence of implant transmucosal design on early peri-implant tissue responses in beagle dogs. *Clin Oral Implants Res.*2014;25:962–968.

16. Kilkenny C, Browne WJ, Cuthill IC, et al. Improving bioscience research reporting: The ARRIVE guidelines for reporting animal research. *PLoS Biol.* 2010;8:e1000412.

17. Donath K, Breuner G. A method for the study of undecalcified bones and teeth with attached soft tissues. The Säge-Schliff (sawing and grinding) technique. *J Oral Pathol.* 1982;11:318–326.

18. Boivin G, Meunier PJ. Histomorphometric methods applied to bone. In: Grupe G, Garland AN, eds. *Histology of Ancient Human Bone: Methods and Diagnosis*. Berlin, Germany: Springer Verlag; 1993:137–156.

19. Cohen J. The concepts of power analysis. In: Cohen J, ed. *Statistical Power Analysis for the Behavioral Sciences*. 2nd ed. Hillsdale, NJ: Erlbaum; 1988:1–17.

20. Finelle G, Papadimitriou DEV, Souza AB, et al. Peri-implant soft tissue and marginal bone adaptation on implant with non-matching healing abutments: Micro-CT analysis. *Clin Oral Implants Res.* 2015;26:e42–e46.

21. Buser D, Weber HP, Donath K, et al. Soft tissue reactions to non-submerged unloaded titanium implants in beagle dogs. *J Periodontol.* 1992;63:225–235.

22. Ruggeri A, Franchi M, Marini N, et al. Supracrestal circular collagen fiber network around osseointegrated nonsubmerged titanium implants. *Clin Oral Implants Res.* 1992;3:169–175.

23. Rodriguez X, Vela X, Calvo-Guirado JL, et al. Effect of platform switching on collagen fiber orientation and bone resorption around dental implants: A preliminary histologic animal study. *Int J Oral Maxillofac Implants.* 2012;27:1116–1122.

24. Degidi M, Piatelli A, Scarano A, et al. Peri-implant collagen fibers around human cone Morse connection implants under polarized light: A report of three cases. *Int J Periodontics Restorative Dent.* 2012;32:323–328.

25. Wennerberg A, Albrektsson T. Effects of titanium surface topography on bone integration: A systematic review. *Clin Oral Implants Res.* 2009;20(suppl 4):172–184.

26. Berglundh T, Abrahamsson I, Lang NP, et al. De novo alveolar bone formation adjacent to endosseous implants. *Clin Oral Implants Res.* 2003;14:251–262.

27. Froum S, Tarnow D, Jalbout Z, et al. Histological evaluation of the Serf EVL evolution, implant: A pilot study in a dog model. *Implant Dent.* 2003;12:69–74.

28. Wennerberg A, Hallgren C, Johansson C, et al. A histomorphometric evaluation of screw-shaped implants each prepared with two surface roughnesses. *Clin Oral Implants Res.* 1998;9:11–19.

29. Welander M, Abrahamsson I, Berglundh T. Subcrestal placement of two-part implants. *Clin Oral Implants Res.* 2009;20:226–231.

30. Cochran DL, Bosshardt DD, Grize L, et al. Bone response to loaded implants with non-matching implant-abutment diameters in the canine mandible. *J Periodontol.* 2009;80:609–617.